Fast electron generation for X-ray production in ultrashort laser interactions with solids

L.A. Gizzi[*], M. Galimberti[*], A. Giulietti[*], D. Giulietti[*,†], P. Köster[*,†], L. Labate[*,**] and P. Tomassini[*]

[*]*Intense Laser Irradiation Laboratory - Istituto per i Processi Chimico-Fisici (CNR), Pisa (Italy) and INFN, Pisa (Italy)*
[†]*Also at: Dipartimento di Fisica "E. Fermi" - Università di Pisa (Italy)*
[**]*Also at Laboratori Nazionali di Frascati, Istituto Nazionale di Fisica Nucleare (Italy)*

Abstract. This article reports on the study of fast electron generation leading to X-ray emission from femtosecond laser interaction with solids presently in progress at the Intense Laser Irradiation Laboratory. The femtosecond laser source and custom developed diagnostics for the characterization of the fast electrons as well as of the X-ray emission is first introduced. Experimental results obtained from the irradiation of Titanium foils are presented. The dependence of the X-ray emission yield on the polarization of the laser light is also showed. Data from the electron diagnostics are then discussed, which shows the presence of energetic electrons accelerated in the forward direction normally to the target surface. Finally, these data are briefly compared with first results from hydrodynamic and PIC simulations.

Keywords: <Enter Keywords here>
PACS: <Replace this text with PACS numbers; choose from this list:

INTRODUCTION

Laser-plasmas are well-known for their X-ray emission properties (see [1] and references therein). The development of powerful femtosecond laser systems based on the Chirped Pulse Amplification (CPA) technique [2] has opened a new interaction regime characterized by high laser intensity and ultrashort pulse duration, which leads to the production of X-ray radiation in the keV energy range due to inner shell transitions in the target material. In principle, X-ray pulses with a duration comparable with the laser pulse duration and source size comparable with the laser focal spot size can be achieved [3, 4, 5].

The primary process for X-ray production from intense CPA laser irradiation of solids is the generation of hot electrons. Several mechanisms can lead to the generation of a population of fast electrons. For the interaction parameters typical of our experimental regime resonant absorption is expected to be the dominant absorption mechanism [6, 7]. In the case of p-polarized laser radiation, efficient energy transfer of laser energy to the plasma can occur [9], giving rise to longitudinal electrostatic electron plasma waves. The subsequent damping of the electron plasma wave, occurring through collisionless damping processes, leads to the generation of a population of electrons having a temperature of tens to hundreds of keV. These energetic electrons can penetrate into the underlying cold target material, where they knock out electrons preferentially from the inner electronic shells of the atoms. The radiative transitions of electrons from the outer

CP827, *Superstrong Fields in Plasmas: Third International Conference on Superstrong Fields in Plasmas*, edited by D. Batani and M. Lontano

shells finally leads to the generation of characteristic K lines.

In this paper a study of the fast electron generation leading to the K shell ionization and consequent X-ray production in solids at intensities above $10^{16}\,\mathrm{W/cm^2}$ is discussed. In the following section the basic diagnostics for the detection of the X-ray emission from the plasma as well as of the fast electrons generated in the forward direction is introduced. Then the experimental results obtained using these diagnostics are discussed and the first results from PIC simulations of the plasma are presented.

THE EXPERIMENTAL SETUP

A schematic view of the experimental setup is shown in Figure 1.

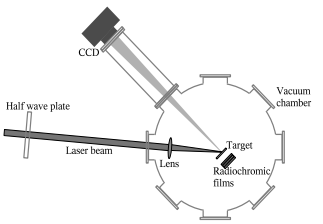

FIGURE 1. Schematic view of the experimental setup.

The laser source is based on a Ti:Sa CPA laser system delivering a pulse with duration $\lesssim 80\,\mathrm{fs}$ and an energy up to 15 mJ at the repetition rate of 10 Hz.

The temporal and spatial properties of the femtosecond pulses have been characterised in detail using custom developed devices. The temporal profile of the pulse was measured with a second order auto-correlator [8]. The autocorrelation curve obtained from a scan of the delay of approximately 1 ps around the maximum SH signal is shown in Figure 2 left. The data points fitted with a double Gaussian function, to take into account the low intensity tails of the curve, yield a FWHM of 67 fs.

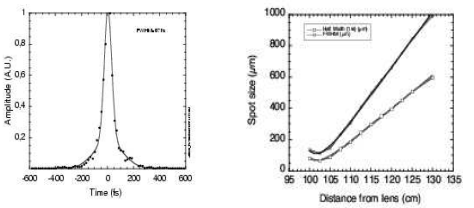

FIGURE 2. (left) Autocorrelation trace of the laser pulse at full amplification. The trace was fitted with a double Gaussian function to account for the real pulse shape. (right) FWHM of the laser beam as retrieved at different distances from a 100 cm nominal focal length lens. A fit with the function for a gaussian beam is also shown.

The spatial quality of the laser pulse has also been studied by means of an equivalent plane monitor (EPM) based on a 100 cm nominal focal length optics and a 12 bits CCD camera (Photometrics Sensys) with a pixel size of 8 μm. The plot of Figure 2 right shows the FWHM of the focused laser spot versus distance, for the 1 meter focal length lens. A fit for this quantity using the function for a Gaussian beam is also shown.

Both the temporal and spatial data show a high quality femtosecond pulse, focusable in a spot size very close to the diffraction limit. According to this result, the FWHM of the pulse best focus for the 100 cm optics is approximately 100 μm. Scaling this value to the 14 cm focal length typically used in our experiments, we can assume a FWHM focal spot of approx. 15 μm. Considering the pulselength of 67 fs and an energy of 15 mJ we find that the peak intensity on the target can reach values of 5×10^{16} W/cm^2.

The laser pulse is focused with an f/20 lens onto the surface of a 12.5 μm thick foil target at an angle of incidence of about 40°. We observe that with our focusing optics, the Rayleigh length is approximately 400 μm, that is, much longer than the expected longitudinal extent of the interaction region. The small portion of the laser beam reflected from the entrance window of the vacuum chamber is sent to a photodiode in order to monitor the single pulse energy. The target foil can be moved horizontally and vertically to ensure a fresh interaction surface for each laser pulse in the series of multi shot measurements.

The X-ray emission generated in the interaction was measured using two types of spectrometers. The first one is based upon a backilluminated cooled CCD placed at about 1 m from the X-ray source and used in single photon mode [10]. This detection technique enables the simultaneous measurement of the spectral properties as well as of the incident X-ray flux. Therefore, it allows a reliable estimate of the X-ray photon yield to be made without independent calibration. In addition, an X-ray spectrometer based on a spherically bent Mica crystal with radius of curvature $R = 150$ mm was used. The crystal was used in the fifth order of diffraction with an angle of incidence at the center of the crystal of about 43°. This spectroscopic technique produces high resolution spectra. In this way, contributions to the X-ray emission from different transitions (not discussed in this paper) could be resolved.

The fast electrons generated during the interaction and passing through the Ti foil were detected by means of a stack of radiochromic films placed at about 5 mm behind the target. The energy of the detected electrons could be retrieved by means of an original reconstruction algorithm [11] based upon a Montecarlo simulation which employes the CERN library GEANT 4.2.0. In particular, two radiochromic layers were used in our case, embedded in an Al pack. We notice here that energetic particles impinging onto the radiochromic films were identified as electrons since the usage of proton sensitive CR39 films lead to a null result.

EXPERIMENTAL RESULTS ON THE X-RAY EMISSION

For the laser parameters of our experiments, the absorption of the laser light is expected to be mainly due to resonance absorption [6]. This absorption mechanism is active when a component of the electric field of the laser light exists along the normal to the critical density surface. Therefore, resonance absorption is strongly dependent on the polarization.

For the experimental study of the dependence of the X-ray yield on the laser light polarization a half wave plate was inserted in the laser beam before the focusing optics. The laser light is p-polarized at the exit of the laser system. Rotating the half wave plate, the polarization of the laser radiation can be rotated continously from p to s. In the

experiment, the polarization was changed stepwise from p to s and again to p. For each rotation angle, the X-ray emission was detected with the CCD for 15 single pulses. For each acquired frame, the signal of all pixels was summed up.

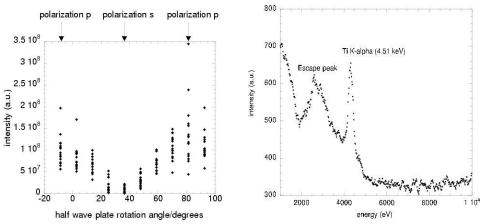

FIGURE 3. (left) X-ray signal as a function of the rotation angle of a half wave plate placed on the laser beam before the focusing optics. The laser light is p-polarized for rotation angles of 81.4° and -8.6° and s-polarized at 36.4°. (right) Spectrum of the X-ray emission produced during the irradiation of a solid Ti target by a 67 fs laser pulse at an intensity above 10^{16} W/cm^2.

This values is plotted in Figure 3 left as a function of the rotation angle of the half wave plate and the angles corresponding to p-polarized and s-polarized laser light are indicated. A strong dependence of the X-ray signal on the polarization of the laser light is clearly visible, being more than one order of magnitude higher for p-polarized laser light with respect to s-polarization. This result indicates that resonance absorption may be playing the dominant role in the absorption of laser radiation for our experimental conditions.

As already discussed in the previous section, the spectral properties of the X-ray radiation emitted during the interaction have been studied by means of a CCD detector working in single photon mode. In fact, it is now well established [10] that each event detected by the CCD can be analysed to retrieve the actual charge produced in the CCD pixels. This charge can then be converted into the incident X-ray photon, via independent energy calibration. A typical spectrum of the X-ray emission (around the K_α line of Titanium at 4.51 keV) is shown in Figure 3 right. The main line visible in the spectrum is the Ti K_α line. At the high energy side of the K_α line the K_β line at 4.93 keV is just visible. Taking into account the solid angle of view of the CCD detection area and assuming an isotropic distribution of emission, we find out that our X-ray source emits approximately 10^7 photons per pulse at a photon energy of 4.51 keV. Since the source can operate at a repetition rate of 10 Hz, that is the rep-rate of the driving laser pulse, we estimate an average X-ray power of 70 nW. X-ray spectra obtained using the bent mica crystal, allowing a study of the emission with a higher spectral resolution have also been studied. A discussion of these spectra will be given elsewhere [12].

EXPERIMENTAL RESULTS ON THE FAST ELECTRON GENERATION AND PRELIMINARY SIMULATIONS

The first of a stack of 2 layers of radiochromic films obtained from a sequence of 100 p-polarized laser shots is shown in Figure 4 right. The darker circular spot is due to a direct irradiation of the film by the laser light eventually due to a burnthrough of the laser in some shots. Indeed, this spot is in the direction of the laser beam, i.e. at around

40° with respect to the target normal. Additionally, a broader, lighter spot can be seen in the lower part of the RC film image. According to the geometry of the experiment, this emission corresponds to the direction of the target normal. This spot clearly shows the presence of energetic electrons accelerated in this direction and passing through the target. The energy of these electrons was estimated by means of Montecarlo simulations that account for energy release in the RC film layers. Figure 4 left shows the energy released in the first two layers of the stack as retrieved by Montecarlo simulations. According to these plots, an energy up to some hundreds of keV can be estimated for the electrons emitted forward and perpendicular to the target surface visible in the Figure.

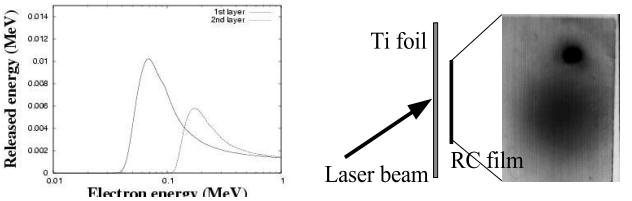

FIGURE 4. (left) Energy released in the 2 radiochromic layers by electrons of different energies as retrieved by Montecarlo simulations. (right) Image of the first layer of an exposed radiochromic film.

As it is well known (see for example [13] or [14]) the production of a hot electron population with a characteristic temperature up to some hundreds of keV is a basic issue in the interaction of ultrashort laser pulses with solids at our intensity. Depending on the dominant mechanism leading to the production of these electrons (such as resonance absorption, ponderomotive heating, etc.), different scaling laws can be found for the temperature as a function of the laser intensity [15, 16]. In our case, resonance absorption can be considered as the most effective process. This has been confirmed by our PIC simulations. The study of the distribution of the penetration angles of these electrons is of a crucial concern when the size of the K_α emitting region is to be considered. This is a quite complex task as it depends upon a number of parameters. In order to understand the physical processes that lead to the production of the electrons detected with our diagnostics, simulations by means of a PIC code have been carried out. Here we show some preliminary results obtained assuming that the interaction occurs with a plasma preformed by the low-level amplified spontaneous emission (ASE). We assumed an ASE intensity on target of $5 \times 10^{10}\,\mathrm{W/cm^2}$ which, according to hydrodynamic simulations, gives a plasma density scalelength at the critical density equal to about $5\,\mu$m. As an example, Figure 5 shows the simulated distribution of the electrons generated in our experimental conditions just after the laser pulse has reached the critical density surface. As it is clearly visible, most of the electrons have their momentum parallel to the target surface. The production of energetic electrons along this direction has been recently observed experimentally in similar conditions to those considered here [17].

Ongoing simulations are aimed at identifying the physical mechanisms capable of explaining the observed production of the hot electrons propagating forward, perpendicular to the target plane. A crucial issue to this purpose is the simulation of the hydrodynamics of the plasma produced by either the ASE or the ps pedestal preceding the main pulse.

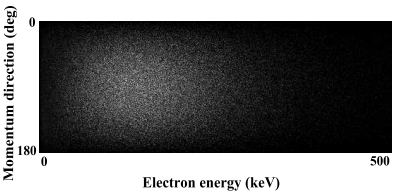

FIGURE 5. Electron distribution as a function of the momentum direction and the energy as retrieved by PIC simulations in our experimental conditions. In this plot, the angle "0" corresponds to electrons propagating along the target normal. Both the horizontal and vertical scales are linear.

SUMMARY AND CONCLUSIONS

A description of the experimental work recently carried out at ILIL related to the setup of an ultrashort X-ray source based on the K_α emission from solid targets has been given. In particular, the issues related to the production of the hot electron population, which is responsible for the X-ray emission, have been studied using diagnostics for both the X-ray emission and the forward accelerated electrons. X-ray emission yield clearly demonstrates that the most effective absorption mechanism is resonance absorption. Electrons having energies up to some hundreds of keV and passing through the Ti foil have been observed both experimentally and numerically. A study of the mechanisms responsible for their production and of their angular distribution is still ongoing, based on hydrodynamic and PIC simulations.

ACKNOWLEDGEMENTS

We would like to thank A. Barbini, A. Rossi, W. Baldeschi and M. Voliani for their invaluable technical assistance. This work was partially supported by the MIUR project 'Impianti innovativi multiscopo per la produzione di radiazione X e ultravioletta'.

REFERENCES

1. D. Giulietti, L.A. Gizzi, *La Rivista del Nuovo Cimento* **21**, 1 (1998)
2. D. Strickland, G. Mourou, *Opt. Commun.* **56**, 219 (1985)
3. C. Reich, P. Gibbon, I. Ushmann, E. Förster, *Phys. Rev. Lett.* **84**, 4846 (2000)
4. F. Ewald, H. Schwoerer, R. Sauerbrey, *Europhys. Lett.* **60**, 710 (2002)
5. T. Feurer, A. Morak, I. Ushmann, C. Ziener, H. Schwoerer, C. Reich, P. Gibbon, E. Förster, R. Sauerbrey, K. Ortner, C.R. Becker, *Phys. Rev. E* **65**, 016412 (2001)
6. S.C. Wilks, W.L. Kruer, *IEEE Journ. Quant. Electronics* **33**, 1954 (1997)
7. L.A. Gizzi, D. Giulietti, A. Giulietti, P. Audebert, S. Bastiani, J.P. Geindre, A. Mysirowicz, *Phys. Rev. Lett.* **76**, 2278 (1996)
8. M. Galimberti, IPCF-CNR Internal Report (2004)
9. D. Riley, L.A. Gizzi, A. MacKinnon, S.M. Viana, O. Willi, *Phys. Rev. E* **48**, 4855 (1997)
10. L. Labate, M. Galimberti, A. Giulietti, D. Giulietti, L.A. Gizzi, P. Tomassini, G. Di Cocco, *Nucl. Instrum. Meth. A* **495**, 148 (2002)
11. M. Galimberti, A. Giulietti, D. Giulietti, L.A. Gizzi, *Rev. Sci. Instrum.* **76**, 053303 (2005)
12. P. Köster *et al.*, *to be submitted*

13. Ch. Reich, I. Ushmann, F. Ewald, S. Düstere, A. Lübncke, H. Scwoerer, R. Sauerbrey, E. Förster, *Phys. Rev. E* **68**, 056408 (2003)
14. H. Nishimura, T. Kawamura, R. Matsui, Y. Ochi, S. Okihara, S. Sakabe, F. Koike, T. Johzaki, H. Nagatomo, K. Mima, I. Ushmann, E. Förtser, *Journ. Quant. Spectr. Radiat. Transfer* **81**, 327 (2003)
15. D. Salzmann, C. reich, I. Ushmann, E. Förster, P. Gibbon, *Phys. Rev. E* **65**, 036402 (2002)
16. D. Riley, J.J. Angulo-Gareta, F.Y. Khattak, M.J. Lamb, P.S. Foster, E.J. Divall, C.J. Hooker, A.J. Langley, R.J. Clarke, D. Neely, *Phys. Rev. E* **71**, 016406 (2005)
17. R. Tommasini, E.E. Fill, R. Bruch, G. Pretzler, *Appl. Phys. B* **79**, 023 (2004)